Egyptian Journal of Archaeological and Restoration Studies (*EJARS*)
An international peer-reviewed journal published bi-annually
www.ejars.sohag-univ.edu.eg

*Original article*

# CHARACTERISTICS OF STUCCO EMPTIER IN AL-ZAHIR BAYBARS AL-BANDAQDARI MOSQUE, CAIRO, EGYPT

Abdelrahim, Sh.[1], Mohammad, A.[1], Fouad, O.[2], Geioushy, R.[2] & Afifi, H.[3(*)]

[1]*Restoration dept., Faculty of Archaeology, Fayoum Univ., Fayoum, Egypt*
[2]*Nanostructured Materials & Nanotechnology dept., Central Metallurgical Research & Development Institute, Cairo, Egypt.*
[3]*Conservation dept., Faculty of Archaeology, Cairo Univ., Giza, Egypt*
**E-mail address: saa00@fayoum.edu.eg*

**Article info.**

**Article history:**
Received: 2-1-2025
Accepted: 4-12-2025
Doi: 10.21608/ejars.2026.511046

**Keywords:**
*Stucco*
*Al-Zahir Baybars Al-Bandaqdari*
*Emptier*
*XRF*
*XRD*
*A stereo microscope*
*SEM.*

EJARS – Vol. 16 (1) – June 2026: 43-48

**Abstract:**

*Sultan Al-Zahir Baybars Al-Bandaqdari established his mosque in (1260-1277 AD), Ghamra, Cairo. The goal of this study is to examine the composition of the stucco emptier that adorn the mosque, as well as to identify their degradation aspects and the various environmental effects. Additionally, the physical characteristics of these ornamentation elements. Three samples from stucco emptier were collected, coded, and examined using many analytical and investigation techniques. The X-ray fluorescence (XRF) analysis of the collected samples indicated that the samples mainly contain Ca, S, Si, and C elements. X-ray diffraction (XRD) has been used to investigate the crystal structure and mineralogical composition. It revealed that the collected samples are composed mainly of gypsum, anhydrite, and quartz. USB digital microscope, polarizing microscope, and scanning electron microscope (SEM) images show that the surface and the core of the samples are rough with a more porous microstructure. Physical properties: density, porosity, and water absorption were also measured to provide full characteristics of the collected stucco samples. The data indicated that the stucco emptier in Al-Zahir Baybars Al Bandaqdari mosque needs restoration to preserve it, and the findings of this study will help in preparing a stucco emptier completion material of the same archaeological components with a slightly different colour to avoid the confusion of authenticity from the original stucco and restored parts.*

## 1. Introduction

Numerous studies have addressed the types of stucco monuments, deterioration factors, aspects, documentation, and conservation processes through successive civilizations, whether as decorative building materials such as mihrabs, friezes, domes, windows, minarets, cast stones, scagliola, pargetting, and sgraffito or as examples of art displayed in museums as masks, molds, or cartonnage. Studies have been conducted to determine the causes and consequences of deterioration, as well as how to document, treat, and maintain architecture and museum stuccoes [1-6]. The decoration of Arab-Islamic architecture is closely related to Islamic art. Islamic arts have unique characteristics [7-11]. Islamic arts spread and flourished throughout the world during the Islamic periods, especially in the Mamluk era. The Islamic stucco arts are characterized by symmetry, repetition, and usage of various decorative elements such as geometric, floral, and inscription decorations. The Mamluk period is considered one of the most significant periods in the history of Islamic architecture in Egypt. The mosque ranks first in the antiquities of Mamluk Bahri in Egypt. The oldest mosques established in Egypt in the era of the Mamluk Bahari (648-784 AH/1250-1382AD) [12,13] date back to 667AH/1268AD. The mosque of Al-Zahir Baybars is one of them, located in the Al-Zahir neighborhood northwest of the northern Cairo wall. Figure (1) shows a general view of the Al-Zahir Baybars Al-Bandaqdari mosque in Cairo. It has two minarets, but it is distinguished by three huge entrances that stand out from the zenith of the mosque's wall with decorations inspired by the entrance to the Al-Aqmar mosque. King Al-Zahir Baybars started to build this mosque in the year 665 AH on the field where he played ball. He completed it in 667AH and made the rest of the square a park inside the mosque. The French have taken a fortress, as Al-Jabarti says, transforming its minaret into a tower and placing cannons. A 1250 m length of sides is about 106 m×103 m, and the height is 12.92 m [14]. In this study, we document, examine, and evaluate a few damaged window wall stucco samples that were gathered from the Al-Zahir Baybars mosque in Cairo, which dates back to the Mamluk era. Various analytical techniques were used to det-ermine the chemical composition of the top surface layer, bulk core, and mortar samples. In addition, the surface and core morphologies have been investigated via stereo-optical, polarizing light, and scanning electron microscopes. Furthermore, the collected sample's density, porosity, and water

absorption were investigated. The findings will assist in the next study in preparing a stucco completion material for the same archaeological components and improving its properties by incorporating some nanomaterials such as nano-silica to achieve the best material that is damage-resistant and homogeneous in properties with the archaeological parts [15,16].


**Figure (1)** general view of the Al-Zahir Baybars Al-Bandaqdari mosque in Cairo; **a.** before restoration, **b.** after conservation processes

## 2. Materials and Methods

### 2.1. *Collection and coding of samples*

The small samples were collected and coded according to their locations in the stucco emptier as follows: ZB1 refers to the sample taken from the outer parts of the stucco emptier to define the deterioration products as the main step to the examination study. ZB2 refers to sample taken from the core of the stucco emptier to study the crystal structure and its components. ZB3 refers to sample taken from the mortar that is located between the stucco emptier and the wall, specifically the fixing mortar, figs. (2 & 3).

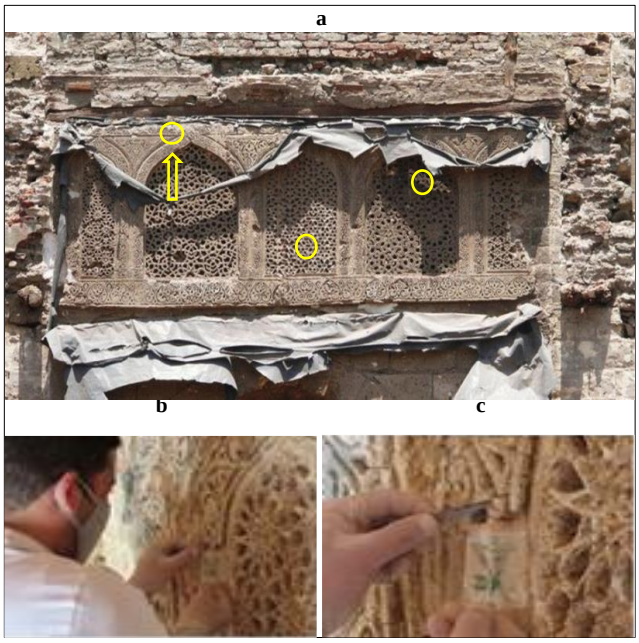


**Figure** (2) **a.** the stucco emptier in Al-Zahir Baybars Al-Banduqdari mosque with sample's location, **b.** & **c.** during samples collection

### 2.2. *Characterization*

The collected samples were examined using analytical and investigative techniques. A portable USB digital microscope camera (20-40X) was used to provide a practical, mobile, and non-destructive method for obtaining high-quality microscopic data and magnified visual observations of deterioration aspects without damaging the stucco emptier [17]. A polarizing light microscope (Leitz Orthoplan, Germany, Digital Camera Leica) at the Mineral Resources and Mining Industries Authority laboratory was used based on the use of polarized light rather than regular light to distinguish the minerals of stucco material through the optical properties of minerals such as shape, color, fracture, cleavage, refractive index, color change, surface topography, morphology, and the interaction between grains and crystals. The scanning electron microscope (SEM, model 200 QUANTA 3D) at the laboratories of the Grand Egyptian Museum was used. X-ray fluorescence analysis as a non-destructive technique was applied to determine the elements constituting the stucco samples qualitatively and quantitatively. X-ray diffraction analysis is used to identify crystal structure and chemical compound composition determination at the Central Metallurgical Research and Development Institute labs. The FT-IR analysis (KBr technique) was used for sample preparation at the Grand Egyptian Museum labs. The spectrum was measured at a resolution of 4 $cm^{-1}$, and 20 scans were recorded per sample. The IR Prestige-21 FTIR spectrometer and the IR solution software at were used. The spectrum in the range 4000-400 $cm^{-1}$ was baseline corrected, and atmospheric compensation was done [18]. Physical characteristics were measured as compressive strength, density, water absorption, and porosity to present full features of the obtained stucco samples.

## 3. Results

### 3.1. *USB digital microscope (LM)*

A portable USB digital microscope investigation showed multiple degradation phenomena on the investigated stucco, including mechanical, chemical, and biological damage: microscopic investigation revealed severe cracking and matrix degradation, fig. (4-a) as indicated by deep vertical fractures and microfractures at the crack edges. This damage was accompanied by disintegration and spalling, fig. (4-b), producing separate surface holes and detached stucco crusts due to physical weathering. Biological deterioration is represented as nests of wasps' remains in the stucco as a biological deterioration affected many open archaeological sites, as shown in figs. (4-c & d).


**Figure (4)** stereo light microscopy images, 40x; **a.** & **b.** macro and micro-cracks, **c.** & **d.** nests of wasps

### 3.2. *Polarizing light microscope (PLM)*

Petrographic analysis of stucco sample Z3, fig. (5-a & b) reveals a dense matrix of microcrystalline gypsum and diffuse calcite hosting a poorly sorted aggregate of small, angular to subangular Qz grains, indicating the use of crushed sand. Microstructural examination, fig. (5-c & d) identifies distinct, oriented pyriform voids with sharp boundary contacts, representing relict porosity footprints left by the degradation of organic binder additives.

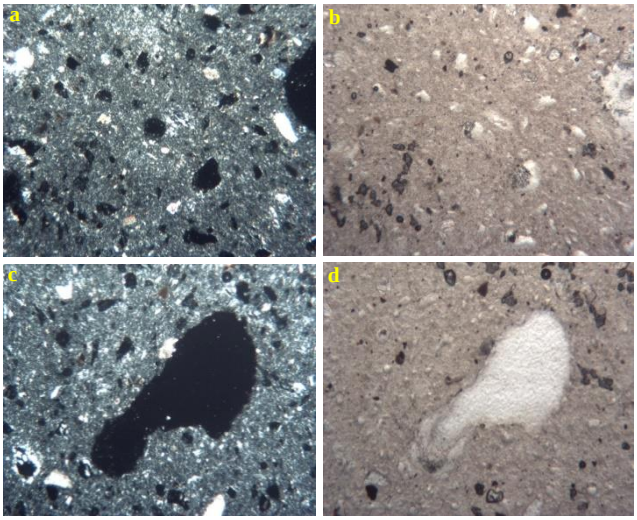


**Figure (5)** the petrographic images showed structure in both normal and polarized light, with gypsum grains as the main component, diffuse calcite grains, and sharp-angle quartz grains of small size in polarized light.

### 3.3. *Scanning electron microscopy (SEM)*

SEM micrographs of the stucco sample identified the extent of the change that occurred in the mineral crystals due to various damage factors, which gives a clear vision of the damage, fig. (6-a & b). It declares the surface weak-ness due to voids between granules as a natural ageing. In addition, EDX analysis displays the presence of the main elements such as Ca, Si, O, S, C, K, Al, Mg, and Fe. The origin of other elements such as K, Al, Mg, and Fe might be due to contamination of the stucco decoration raw materials or because of environmental impact on the archaeological monuments.

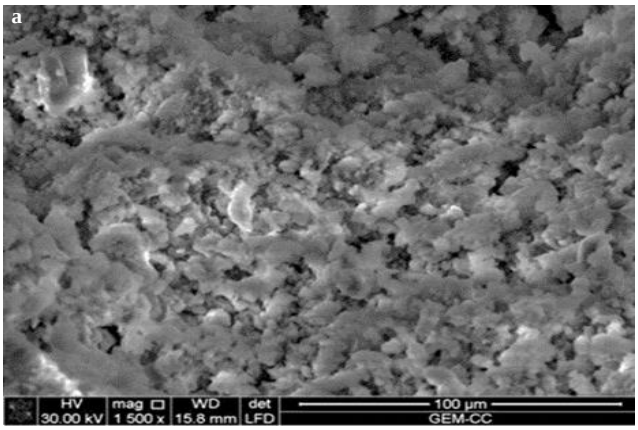


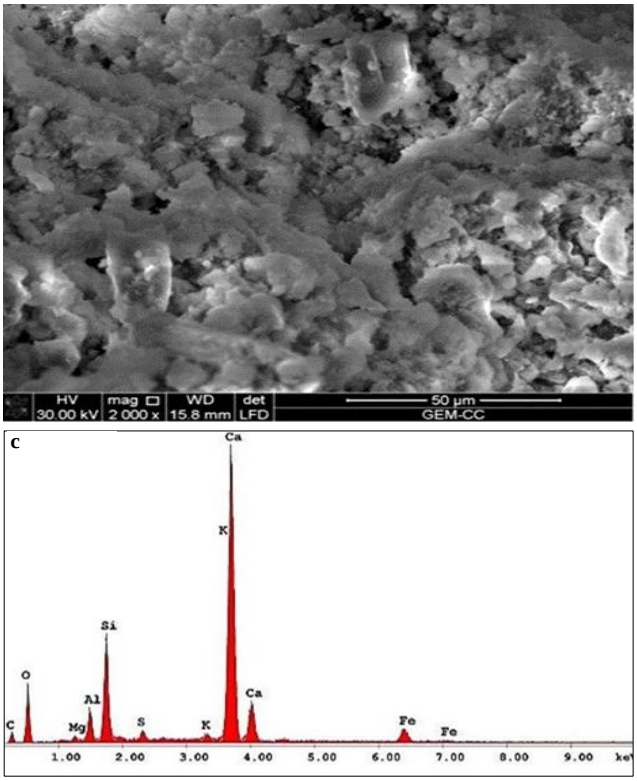


**Figure (6)** **a.** & **b.** SEM photomicrographs of the selected stucco sample, **c.** EDX pattern of the same sample

### 3.4. *Portable Energy-dispersive X-ray fluorescence analysis (pEDXRF)*

Table (1) shows the data collected from XRF analysis of the two stucco samples (surface and core). The results reveal that the main constituting elements are S and Ca, which refer to calcium sulfate as the main component in the stucco sample and quartzite minerals. The presence of carbon C indicates that air pollutants are accumulated on the archaeological surface of the stucco samples.

**Table (1)** XRF analysis of the selected stucco samples

| Oxide | Surface sample | Core sample |
|---|---|---|
| **$SO_2$** | 18,35 | 9,97 |
| **CaO** | 70,72 | 80,71 |
| **SrO** | 0,20 | 0,43 |
| **$Fe_2O_3$** | 2,41 | 1,22 |
| **$TiO_2$** | 0,23 | 0,12 |
| **$K_2O$** | 0,56 | 2,71 |
| **$SiO_2$** | 6,49 | 1,48 |
| **$CO_2$** | 0,13 | 3,36 |
| **ZrO** | 0,005 | - |
| **PbO** | 0,05 | - |
| **ZnO** | 0,02 | - |
| **$Al_2O_3$** | 0,83 | - |
| **$V_2O_5$** | 0,01 | - |
| **Total** | **100%** | **100%** |

### 3.5. *X-ray diffraction analysis (XRD)*

Figure (7) shows the chemical compound composition of the collected stucco samples (ZB1, ZB2, and ZB3) analyzed by XRD. Obviously, it is clear that all samples composed mainly of four chemical compounds; calcium sulfate hydrate (gypsum, $CaSO_4.2H_2O$), calcium sulfate (anhydrite, $CaSO_4$), silica

(quartz, $SiO_2$) and calcium carbonate (calcite, $CaCO_3$). Semi-quantitative analysis of the detected chemical compounds is also represented in tab. (2). The semi-quantitative analysis of the first two samples (ZB1 and ZB2) is close to each other. While the semi-quantitative analysis of the third sample (ZB3) is clearly different in the percentage of gypsum, anhydrite, and calcite. This might be due the effect of surrounding environment and the air pollution around the archaeological open sites [19]. This is obvious by decreasing the proportion of gypsum to 54% compared with 70 and 64.6% for the other two samples. The amount of anhydrite rose to 36%, compared to 20% and 25% in the other two samples. It is proof of the interaction between the gypsum compound and the surrounding environment, as well as the occurrence of deterioration and the passing of the impact over an exten-ded length of time, creating chemical compounds to be altered. Calcite is added to the gypsum compound to extend its sol-idification period, and quartz is utilized as filler in stucco material.

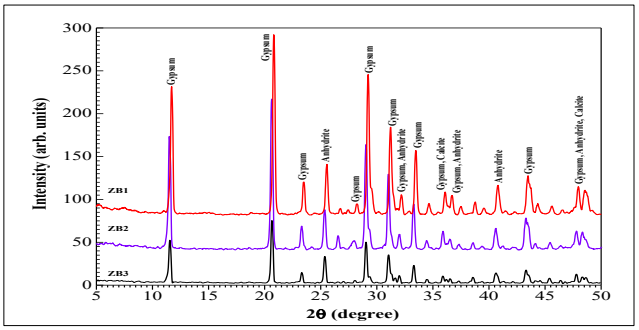


**Figure (7)** XRD patterns of the three stucco emptier samples

**Table (2)** mineralogical compound composition by XRD analysis of selected stucco samples of the monument

| Compound | Chemical Formula | Semi quantitative (%) | | |
|---|---|---|---|---|
| | | *(ZB1)* | *(ZB2)* | *(ZB3)* |
| **Gypsum** | $CaSO_4.2H_2O$ | 70 | 64.6 | 54 |
| **Anhydrite** | $CaSO_4$ | 20 | 25.3 | 36 |
| **Calcite** | $CaCO_3$ | 8 | 8.3 | 10 |
| **Quartz** | $SiO_2$ | 2 | 2.5 | -- |

### 3.6. *Fourier transform infra- red analysis (FT-IR)*

The broadness and specific positions of the carbonate absorption bands 1317-1384 $cm^{-1}$ and out-of-plane bending near 781 $cm^{-1}$, fig. (8) suggest that the identified calcite is a secondary product formed through the carbonation of a lime-based binder, rather than the use of primary crushed limestone as a filler. Sulfate stretching bands between 1109-1163 $cm^{-1}$ and bending modes at 601–669 $cm^{-1}$ confirm the presence of gypsum. The FT-IR spectrum of sample ZB1 exhibits a broad OH stretching band between 3244-3594 $cm^{-1}$, which is consistent with the structural water present in gypsum. While a sharp OH band near 3640 $cm^{-1}$ would be required to confirm residual $Ca(OH)_2$ and thus a burnt lime origin, the current spectrum more clearly supports the presence of gypsum alongside calcite phases. Furthermore, the FT-IR spectra were essential for screening the samples for any residual organic binders, such as linseed oil or animal glues, which are historically known to be added to stucco to improve plasticity. The absence of characteristic C-H and C=O stretching bands in the organic regions (around 2850-2950 $cm^{-1}$ and 1700-1740 $cm^{-1}$) confirms that these specific samples were formulated using a purely inorganic mineral system, providing a clear understanding of the original recipe and its long-term stability.

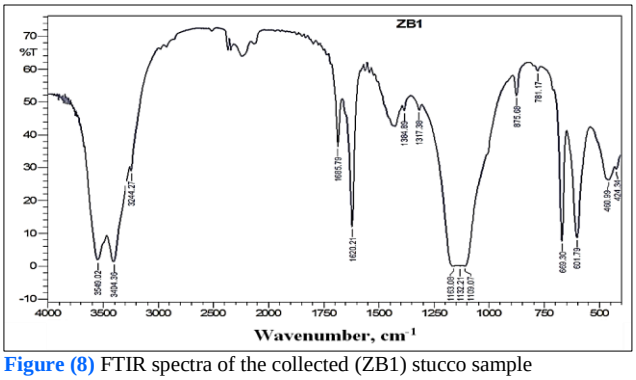


**Figure (8)** FTIR spectra of the collected (ZB1) stucco sample

### 3.7. *Physical characteristics*

Due to the historical nature of the stucco emptier, mechanical testing was performed on representative fragments (sub standard dimensions) for fragile stucco materials. The compressive strength, density, and water absorption and porosity of the selected pieces of stucco emptier -*left for study*- were measured and evaluated as listed in tab. (3), It is clear that it has a low compressive strength (12.13 $kg/cm^2$) with high water absorption (61.10%) and relatively high porosity (52.83%).

**Table (3)** the physical characterization of the (ZB2) sample

| Sample Code | Compressive strength ($Kg/cm^2$) | Water absorption (%) | Density ($g/cm^3$) | Porosity (%) |
|---|---|---|---|---|
| Stucco fragment (ZB2) | 12.13 | 61.10 | 0.87 | 52.83 |

## 4. Discussions

The integrated analytical results offer comprehensive insight into the composition, microstructure, and deterioration mechanisms of the stucco emptier at Al-Zahir Baybars mosque. The biological deterioration of stucco by nests of wasps' remains was observed by the portable USB digital microscope [19]. In all samples gypsum ($CaSO_4.2H_2O$) is the dominant mineral confirming its historical role as the primary binder, aligning with Mamluk architectural practices where gypsum was favored for its rapid setting and high plasticity in intricate carvings [6]. However, the detection of anhydrite ($CaSO_4$), particularly in the mortar layer (ZB3), suggests a significant partial thermal transformation from dihydrated gypsum to the dehydrated phase. This phase transition is likely a technological marker of the original calcination process or a result of centuries of exposure to Cairo's hyper-arid environmental fluctuations and high-temperature cycles, which agreed with Afifi, et al. [20] and Abdelrahim, et al [23]. The presence of calcite ($Ca\ CO_3$) further deepens the understanding of the material's change. While it could be viewed as a simple filler, the specific carbonate bonding observed in FT-IR, along with the absence of geogenic limestone textures in PLM suggests a more complex role for the calcite [24-28]. It was suggested that this calcite is primarily a carbonation product. This indicates a sophisticated "composite binder" technology where a

small amount of lime was likely added to the gypsum to moderate the setting rate and improve long-term durability. The presence of quartz ($SiO_2$) aggregates further supports this mineralogical coupling [29-32]. As revealed by XRD, PLM, and SEM, the use of siliceous sand provided a mechanical skeleton for the matrix; however, the current low compressive strength indicates that this internal skeleton has been compromised over time. Microscopic and SEM observations reveal a highly porous (52.83%) and heterogeneous microstructure, with clear signs of advanced physical and chemical degradation. The observed micro-cracks and grain detachment are merely age-related by environmental deterioration factors. The presence of sulfur and carbon in EDX and XRF spectra supports the hypothesis that urban atmospheric pollutants play a key role in the deterioration process [33]. These pollutants react with the calcium phases within the stucco to form damaging secondary sulfate salts, creating internal pressures that lead to the "exfoliation" of the decorative surface [34]. These findings confirm that the original stucco, although skillfully prepared, has undergone progressive alteration due to both intrinsic material characteristics and extrinsic environmental pressures. The excessive water absorption (61.10%) further accelerates this decay by facilitating the capillary rise of groundwater salts. From a conservation standpoint, these results underscore the necessity of adopting compatible material and minimally invasive interventions. Restoration stucco must emulate this mineralogical profile to ensure cohesion and prevent future detachment. Nano-enhanced treatments, such as nano-lime or nano-silica, offer promising solutions by improving mechanical strength and reducing porosity; however, their long-term behavior under the specific urban pollution profile of Cairo must be carefully evaluated to ensure the survival of this Mamluk masterpiece.

## 5. Conclusion

*Characterization of the stucco emptier from the Al-Zahir Baybars Al-Bandaqdari mosque reveals a complex interplay between historical craftsmanship and aggressive environmental decay. Mineralogical profiling identifies gypsum ($CaSO_4.2H_2O$) as the primary historical binder, reflecting Mamluk traditions that valued the material for its rapid setting and fluid workability in detailed reliefs. However, the presence of anhydrite ($CaSO_4$) in the ZB3 mortar layer indicates partial thermal transformation, suggesting either precise control over original calcination temperatures or structural adjustments caused by centuries of exposure to Cairo's hyper-arid thermal cycles. Microstructural analysis refutes the assumption that the detected calcite ($CaCO_3$) is merely an inert filler; the absence of geogenic textures under PLM and the specific carbonate footprints in FT-IR confirm it as a secondary carbonation product. This points to an advanced composite binder technique where Mamluk artisans introduced small amounts of lime to gypsum to modulate setting times and prolong durability. Although siliceous sand aggregates provided the initial mechanical framework, centuries of environmental stress have severely degraded this internal skeleton, leaving the current matrix with negligible compressive strength. Today, the stucco exhibits a highly porous (52.83%) and degraded microstructure. Scanning electron microscopy and spectroscopic data (EDX/XRF) show that urban atmospheric pollutants have driven this decay by reacting with the calcium matrix to form secondary sulfate salts. The resulting internal crystallization pressures, exacerbated by a high-water absorption capacity (61.10%) and persistent capillary moisture rise, are the direct catalysts behind the widespread micro-cracking, grain detachment, and surface exfoliation currently threatening the monument. Remediation requires strict adherence to material compatibility. Developing restoration mortars that match this historical mineralogical fingerprint is vital to prevent future interfacial shearing. Furthermore, while nano-lime and nano-silica interventions offer viable methods for microstructural consolidation and porosity reduction, their long-term resilience against Cairo's aggressive atmospheric pollution must be thoroughly validated to safeguard this architectural masterpiece.*

## References


**[1]** Abdel-Ghani, M., Afifi, H., Mahmoud, R.., et al., (2020). Graeco-Roman Egyptian cartonnage from the Egyptian museum in Cairo, Egypt: Technical and analytical investigation, *J. of Archaeological Science: Reports*. 31, doi: 10.1016/j.jasrep.2020.102360.

**[2]** Afifi, H., Hamed, S., Mohamedy, S., et al., (2019). a dating approach of a refundable wooden Egyptian coffin lid. *Scientific Culture*. 5 (1): 15-22.

**[3]** Caroselli, M., Zumbühl, S., Cavallo, G., et al. (2020). Composition and techniques of the Ticinese stucco decorations from the 16th to the 17th century: results from the analysis of the materials. *Herit Sci*. 8 (1), doi: 10.1186/s40494-020-00446-4.

**[4]** Bartz, W., Kierczak, J., Gąsior, M., et al. (2017) Analytical overview of different Baroque plastering techniques applied in the post-Cistercian abbey in Lubiąż (South-Western Poland). *J. Cult Herit*. (28): 37-47.

**[5]** Afifi, H. & Geweely, N., Galal, H., et al. (2016). Antimicrobial activity of gold nanoparticles (AuNPs) on deterioration of archaeological gilded painted cartonnage, late period, Saqqara, Egypt. *Geomicrobiology. J*. 33 (7), doi: 10.1080/01490451.2015.1062064.

**[6]** Abdelrahim, Sh., Mohammed, A., Afifi, H., et al., (2026). Characterization of the architectural stucco rococo style of El-Sakakini palace facades, Cairo, Egypt (Analytical and investigation study). *Shedet*. 15 (1): 310-324.

**[7]** Almeida, L., Santos Silva, A., Veiga, R., et al. (2023). 20th century mortars: Physical and mechanical properties from awarded buildings in Lisbon (Portugal)—studies towards their conservation and repair. *Buildings*. 13 (10), doi: 10.3390/buildings13102468.

**[8]** Zahra, F. & Shahir, S. (2022). The spiritual aesthetics of Islamic ornamentation and the aesthetic value in Islamic architecture. *J. of Islamic Thought & Civilization*. 12 (1): 133-150.

**[9]** Huseynova, L. (2026). The evolution, philosophy and manifestation of ornaments in Islamic art within sacred spaces: A comprehensive study. *Islamic History & Literature*. 4 (2): 136–144.

**[10]** Corsi, A. (2017). A brief note on early Abbasid stucco decoration: Madinat al-Far and the first Friday mosque of Isfahān. *Vicino Oriente*. XXI: 83-95.

**[11]** Khan, S. (2014). The use of stucco as a medium of decoration a case study of the tomb building of Kaka Sahib, Nowshehra. Pakistan. *Heritage*. 2: 442-448.

**[12]** Mulder, S. (2025). Innovation and transformation in the stucco of Bilad al-Sham. In: McClary, R. (ed.) *Stucco in the Islamic World: Studies of Architectural Ornament from Spain to India*. Edinburgh Univ. Press, Edinburgh, Ch. 7, pp. 131-150.

**[13]** Nikitha, S., Sri-Pranap, K. & Debak, Ar. (2025). A review on evolution of decorative stucco in architecture. *Int. J. of Research Publication & Reviews.* 6 (10): 4540-4547.

**[14]** Al-Jboory, S. (2019). Floral decorations in the Abbasid palace architecture in Baghdad "Analytical study". *An-Najah Univ. J. for Research - B (Humanities)*. 33: 1507-1536.

**[15]** Geweely, N., Afifi, H., Abdelrahim, S., et al. (2014). Novel comparative efficiency of ozone and gamma sterilization on fungal deterioration of archeological painted coffin, Saqqara excavation, Egypt. *Geomicrobiology J.* 31 (6): 529-539.

**[16]** Hamed, E. & Abdel Rahim, S. (2024). The comprehensive practical documentation to one of the spaces of the historical palaces in Cairo for starting conservation work (case study). *Shedet,* 13 (13): 383-397.

**[17]** Shekofteh, A. (2025). Techniques and stylistic characteristics of stucco decorations in Ilkhanid architecture of Iran. *Heritage*. 8 (11), doi: 10.3390/heritage8110443.

**[18]** Sciau, P., Godet, M. & Adriaens, M. (2021). Spectroscopy and diffraction using the electron microscope. In: Adriaens, M. & Dowsett, M. (eds.) *Spectroscopy, Diffraction & Tomography in Art & Heritage Science*, Elsevier, Amsterdam, pp.71-102

**[19]** Geweely, N. & Afifi, H., (2011). Bioremediation of some deterioration products from sandstone of archaeological Karnak temple using stimulated irradiated alkalothermophilic purified microbial enzymes. *Geomicrobiology J*. 28 (1): 56-67

**[20]** Riccardi, M. & Duminuco, P. & Tomasi C. (1998). Thermal, microscopic and X-ray diffraction studies on some ancient mortars. *Thermochimica Acta*. 321 (1-2): 207- 214.

**[21]** Hamm, J. (1986). Review of the conservation of wall painting by P. Mora, L. Mora & P. Philippot. *Bulletin of the Ass-ociation for Preservation Technology*, 18 (3): 69-71.

**[22]** Afifi, H., Galal, H. & Ali Hassan, R. (2020) Characteriza-tion of pharaonic cartonnage from a late period, Saqqara excavations, *Pigment & Resin Technology*. 49 (4): 255-264

**[23]** Basu, D. (2020). Stucco as a building material - a study of its composition, use and scientific analysis. *Heritage*. 8 (2): 662-679.

**[24]** Madejova, J. (2003). FTIR techniques in clay mineral studies: review. *Vibrational Spectroscopy*. 31 (1): 10-19.

**[25]** Al-Amin, K., Kawsar, M., Mamun, M. et al. (2025). Fourier transform infrared spectroscopic technique for analysis of inorganic materials: A review. *Nanoscale Advances*. 7 (21): 6677-6702.

**[26]** Lyman, C., Newbury, I., Goldstein, J., et al. (1990). Scanning *electron microscopy, x-ray microanalysis, and analytical electron microscopy a laboratory* Work-book Plenum Press, NY.

**[27]** Marocchi, M., Dellisanti, F., Maria, G., et al., (2010). SEM-XRD Investigation of deterioration morphologies consolidation prior to restoration: The case of Port a Nuovain Ravenna (Italy). *Periodico di Mineralogia*. 79 (1): 81-93.

**[28]** Moropoulou, A., Zendri, E., Ortiz, P., et al. (2019). Scanning microscopy techniques as an assessment tool of materials and interventions for the protection of built cultural heritage. *Scanning.* 2019, doi: 10.1155/ 2019/5376214.

**[29]** Laforce, B., Vermeulen, B. & Garrevoet, J. (2016). Laboratory scale x-ray fluorescence tomography: Instrument characterization and application in earth and env-ironmental science, *Anal. Chem.* 88 (6): 3386-3391.

**[30]** Janssens, K., Vincze, L. & Vekemans, B. (2021). Adv-ances in X-ray fluorescence imaging for cultural heritage and planetary materials. *Spectrochimica Acta Part B: Atomic Spectroscopy*. 177 (1): 106-118.

**[31]** Vázquez, M, Galan, E., Ortiz, P., et al. (2013). Digital image analysis and EDX SEM as combined techniques to evaluate salt damp on walls. *Construction & Building Materials*. 45 :45-95.

**[32]** Scoot, D. (2001) The application of scanning X-ray fluorescence microanalysis in examination of cultural materials. *Archaeometry*. 43 (4): 475-482.

**[33]** Abdelfattah, A., Ragab, A., Younis S., et al. (2023). Evolution of the physico-mechanical properties of cal-cined clay cement from different sources of kaolin clay. *IRJET J*. 10 (6): 485-497.

**[34]** Mahmoud, H. (2014). Investigations by Raman microscopy, ESEM and FTIR-ATR of wall paintings from Qasr el-Ghuieta temple, Egypt. *Herit Sci*. 2, doi: 10. 1186/s40494-014-0018-x.